AD/A-003 010

INFRARED SPECTROSCOPIC STUDIES OF LOW
PRESSURE ELECTRONIC DISCHARGES

John Strong, et al

Massachusetts University

Prepared for:

Defense Nuclear Agency
Defense Advanced Research Projects Agency
Physical Sciences, Incorporated

25 November 1974

AD/A003010

REPORT DOCUMENTATION PAGE		READ INSTRUCTIONS BEFORE COMPLETING FORM
1. REPORT NUMBER DNA 3433F	2. GOVT ACCESSION NO.	3. RECIPIENT'S CATALOG NUMBER
4. TITLE *(and Subtitle)* INFRARED SPECTROSCOPIC STUDIES OF LOW PRESSURE ELECTRONIC DISCHARGES		5. TYPE OF REPORT & PERIOD COVERED Final Report for Period 15 Jan 73—14 Apr 74
		6. PERFORMING ORG. REPORT NUMBER UMASS-ARF-74-286
7. AUTHOR(s) J. Strong K. L. Wray (PSI) P. Hansen G. E. Caledonia (PSI)		8. CONTRACT OR GRANT NUMBER(s) DNA 001-73-C-0143
9. PERFORMING ORGANIZATION NAME AND ADDRESS Astronomy Research Facility University of Massachusetts Amherst, Massachusetts 01002		10. PROGRAM ELEMENT, PROJECT, TASK AREA & WORK UNIT NUMBERS DARPA Order No. 1433, Amendment No. 7.
11. CONTROLLING OFFICE NAME AND ADDRESS Director Defense Advanced Research Projects Agency Washington, D.C. 20305		12. REPORT DATE 25 November 1974
		13. NUMBER OF PAGES ~~20~~ 21
14. MONITORING AGENCY NAME & ADDRESS(if different from Controlling Office) Director Defense Nuclear Agency Washington, D.C. 20305		15. SECURITY CLASS (of this report) UNCLASSIFIED
		15a. DECLASSIFICATION DOWNGRADING SCHEDULE

16. DISTRIBUTION STATEMENT *(of this Report)*

Approved for public release; distribution unlimited.

17. DISTRIBUTION STATEMENT *(of the abstract entered in Block 20, if different from Report)*

18. SUPPLEMENTARY NOTES

This work sponsored by the Defense Advanced Research Projects Agency under DARPA Order No. 1433, Amendment No. 7.

19. KEY WORDS *(Continue on reverse side if necessary and identify by block number)*

Ozone   Infrared
Electric Discharges   Spectroscopy

20. ABSTRACT *(Continue on reverse side if necessary and identify by block number)*

Emission spectra of low pressure, large volume electronic discharges in air, oxygen, and nitrogen are described. Problems arising from an attempt to observe excited ozone at 9.6μ are discussed in detail. Sample spectra in the 2μ wavelength are presented.

(21)

DD $_{1\ JAN\ 73}^{FORM}$ 1473   EDITION OF 1 NOV 65 IS OBSOLETE

9. PERFORMING ORGANIZATION NAME AND ADDRESS (Continued)

Physical Sciences, Inc.
607 North Avenue
Wakefield, Massachusetts 01880

10. PROGRAM ELEMENT, PROJECT, TASK AREA & WORK
UNIT NUMBERS (Continued)

DARPA Task Code E50, Work Unit No. 01

TABLE OF CONTENTS

1

LIST OF ILLUSTRATIONS

LIST OF TABLES

IR RADIATION MODEL FOR EXCITED OZONE
PRODUCED IN A PURE O_2 ELECTRIC DISCHARGE

Kurt L. Wray and George E. Caledonia

Physical Sciences, Inc.
Wakefield, Massachusetts

Introduction

The theoretical work reported here was done in conjunction with the experimental program being carried out at the Astronomy Research Facility at the University of Massachusetts under the direction of Prof. John Strong. The experimental program, directed at the study of the chemistry of species produced by electrical discharges in a simulated upper atmosphere, is being carried out in a 100 feet long, 3 feet diameter discharge tube. The tube has cylindrical coaxial geometry with the outer wall serving as one electrode and a 33 feet long, 3 inch diameter tube located axially along the central one third of the larger tube serving as the other electrode. The optical system allows triple pass operation and the test gas can be studied in either absorption or emission. Neglecting axial diffusion, the effective optical path for discharge produced species is then 100 feet or 3×10^3 cm.

Experimental Conditions

A visibly uniform discharge was achieved with 600 volts (direct current) at a pressure of 0.1 Torr; the total current, I, drawn under these conditions was 0.3 amp.

The electric field, E, for cylindrical geometry is given by

$$E \approx \frac{V}{r \ln (r_2/r_1)} \approx \frac{V}{2.5r} \tag{1}$$

where $V = 600$ is the potential across the electrodes and $r_1 = 3.8$ cm and $r_2 = 46$ cm, the inner and outer electrode radii, respectively. At a pressure of 0.1 Torr,

$$57 < E/P < 720 \left(\text{volt cm}^{-1} \text{ Torr}^{-1} \right) . \tag{2}$$

In pure O_2 this corresponds to an electron temperature T_e of

$$T_e \gtrsim 2.5 \text{ eV} . \tag{3}$$

If there were no ionization in the gas, the electron concentration n_e would be given by the equation

$$n_e = \frac{I}{2 \pi r 1 \nu Q} \tag{4}$$

where $1 = 1 \times 10^3$ cm is the discharge length and Q is the charge on an electron $(1.6 \times 10^{-19}$ coulomb). The electron drift velocity ν was taken to be $\nu = 2 \times 10^7$ cm/sec as typical for the discharge conditions, hence, for $I = 0.3$ amp

$$n_e \approx 3 \times 10^5 \text{ electrons/cm}^3 \tag{5}$$

at the outer wall. It is probably not much more than a factor of 10 larger than that anywhere in the discharge volume even though the inclusion of gas ionization effects would modify the r^{-1} dependence of Equation (4). In making numerical calculations below, we arbitrarily use

$$n_e \equiv 2 \times 10^7 \text{ electrons/cm}^3 \tag{6}$$

as an upper bound to the local electron concentration in the present experimental apparatus.

Heterogeneous reactions occurring on the walls of the apparatus are important. These are kinetically limited by diffusion of the reactive (neutral) species to the walls. For the system geometry, the characteristic diffusion time τ_{diff} is given by a complex transcendental equation involving Bessel functions; for the actual r_1 and r_2 involved, we find

$$\tau_{diff} \approx 1.5 \text{ P (sec)} \tag{7}$$

where P is the pressure in Torr.

Kinetic Mechanisms

Table I gives the kinetic processes to be considered in a pure O_2 discharge for the experimental conditions discussed above. Also given in Table 1 are the rate constants k for 2- and 3-body reactions 1 through 6, or time constants τ for unimolecular processes 7 through 9. Here we comment on each of the rate constants given in Table 1.

4

Reaction 1: Discussed below.

2: Well known.

3: Recently measured (C. von Rosenberg).

4: Unknown but process probably not important here because both reactants are trace species.

5: Well known.

6: Well known.

7: Diffusion calculation is accurate and $\gamma \approx 1$ is good assumption.

8: γ is unknown but process is unimportant at $P > .03$ Torr even with $\gamma \equiv 1$.

9: Assumes $\tau_R \ (v = 4 \to 3) = \dfrac{\tau_{system}}{4}$

Reaction 1 is listed in Table I as a global reaction. The basis for this can be seen in Figure 1 where the rate constants for the following reactions are plotted vs. E/P.

Reaction 10: $e + O_2 \to O + O^-$

11: $O^- + O_2 \to O + O_2 + e$

12: $e + O_2 \to O_2^+ + 2e$

TABLE 1. PURE O_2 DISCHARGE KINETICS

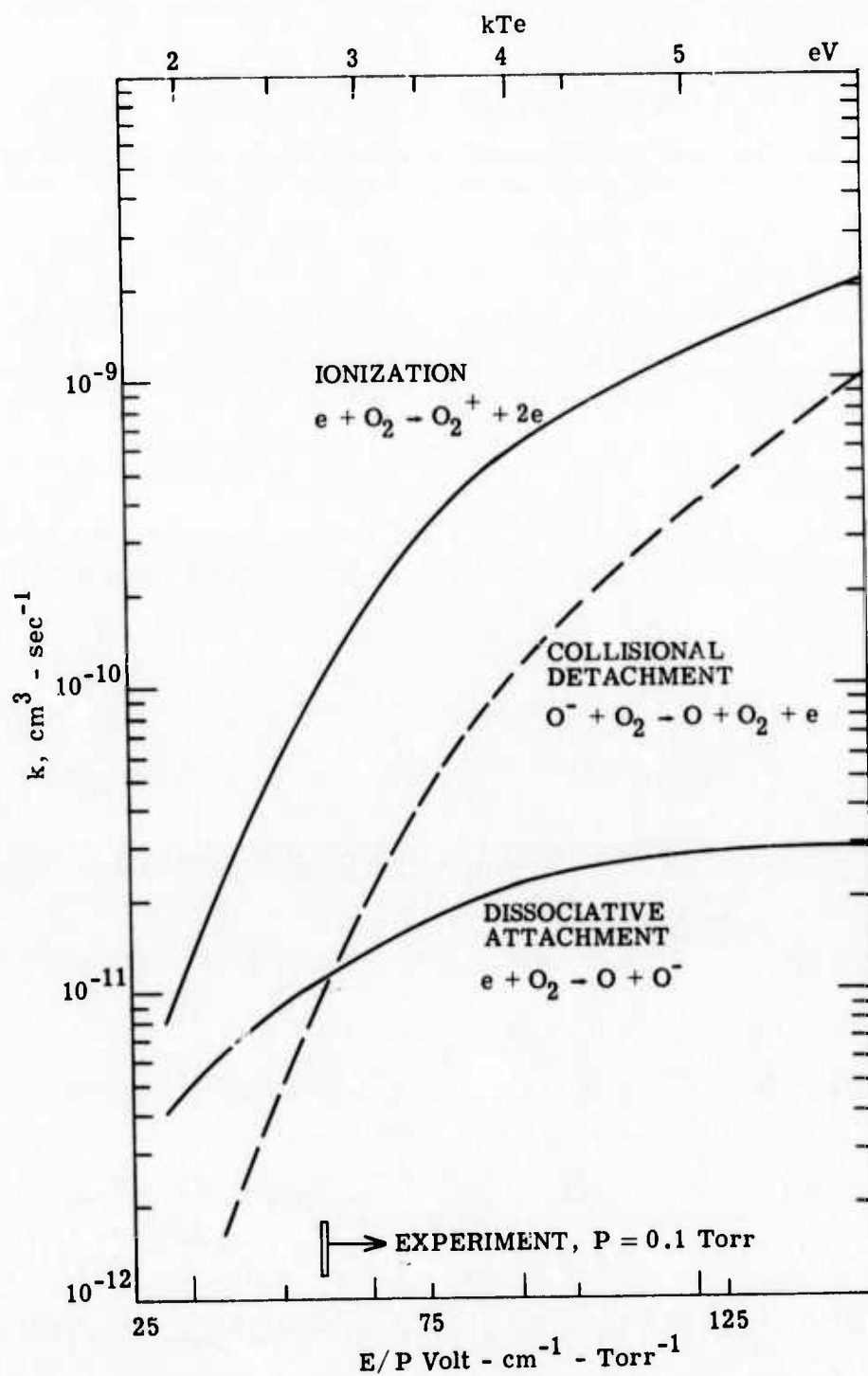| Reaction	Rate constant
1: $e + O_2 \xrightarrow{\text{Global}} 2O + e$	$k = f\,(E/P)\ cm^3\ sec^{-1}$
2: $O + 2O_2 \longrightarrow O_3^* + O_2$	$k = 6 \times 10^{-34}\ cm^6\ sec^{-1}$
3: $O_3^* + O_2 \longrightarrow O_3 + O_2$	$k = 2 \times 10^{-14}\ cm^3\ sec^{-1}$
4: $O_3^* + O \longrightarrow 2O_2$	$k = ?$
5: $O_3 + O \longrightarrow 2O_2$	$k = 6 \times 10^{-15}\ cm^3\ sec^{-1}$
6: $O + O + O_2 \longrightarrow 2O_2$	$k = 5 \times 10^{-33}\ cm^6\ sec^{-1}$
7: $O \xrightarrow[\text{Wall}]{\sigma = 1} 1/2\ O_2$	$\tau_D = 1.5\ P_{Torr}\ sec$ (system)
8: $O_3^* \xrightarrow[\text{Wall}]{} O_3$	$\tau_D = 1.5_\sigma^{-1}\ P_{Torr}\ sec$ ($\sigma < 1$)
9: $O_3^* \longrightarrow O_3 + h\nu$	$\tau_R = 2.5 \times 10^{-2}\ sec$ ($\nu = 4 \to 3$)

*Vibrationally excited.

5

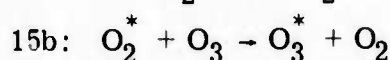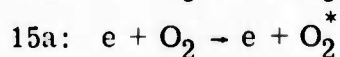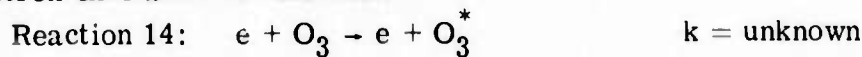Figure 1. Discharge characteristics in pure O_2.

6

It is noted that Reaction 10 is rate limiting; for the E/P range of interest, the O^- produced is rapidly destroyed by collisional detachment, the sum of 11 and 12 being the global reaction 1 with an effective rate constant of $\sim 2 \times 10^{-11}$. Reaction 12 identifies O_2^+ as the dominant positive ion, whose concentration is equal to the electron concentration since negative ions are unimportant here.

We have not included in our model ozone destruction by electrons:

$$\text{Reaction 13:} \quad e + O_3 \Big\langle \begin{array}{l} O^- + O_2 \\ O_2^- + O \end{array}$$
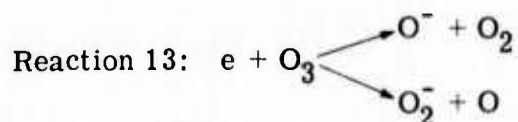
which processes have cross sections $\sigma \sim 10^{-19}$ cm^2 at electron energies ~ 5 eV. This cross section would make Reaction 13 unimportant for $n_e \lesssim 10^8$ cm^{-3}.

Furthermore, we have not included in our model direct (direct or indirect) electron excitation of vibration:

$$\text{Reaction 14:} \quad e + O_3 \rightarrow e + O_3^* \qquad\qquad k = \text{unknown}$$
$$\text{15a:} \quad e + O_2 \rightarrow e + O_2^*$$
$$\text{15b:} \quad O_2^* + O_3 \rightarrow O_3^* + O_2$$

These reactions are not considered to be important--more will be said about Reaction 14 below.

Steady State Solutions

The rate equations for $[O]$, $[O_3^*]$, and $[O_3]$ are given in Table 2. Here $[\ ]$ are mole fractions and N is the total number of particles/cm^3 which is essentially the O_2 concentration. At the bottom of Table 2, complete equations are given for the steady state mole fractions obtained by setting $d[\ ]/dt \equiv 0$. Crossed out terms were shown to be negligible for present conditions. The radiative and catalytic decay of O_3^* are readily shown to be unimportant at the higher pressures; i.e., $P \gtrsim 0.06$ Torr for radiative decay and $P \gtrsim 0.03$ Torr for wall catalysis. Hence at $P \gtrsim 0.06$ Torr, assuming

$$[O] \ll [O_2] \tag{8}$$

and using the rate constants of Table 1, we find (to 1 significant figure)

$$[O] = \frac{3 P k_1 n_e}{1 + \alpha P^3} \qquad \begin{array}{l} \text{catalytic wall} \\ \text{for O-atoms} \end{array} \tag{9}$$

---

* Vibrationally excited.

7

TABLE 2. KINETIC EQUATIONS AND STEADY STATE SOLUTIONS

$$\frac{d[O]}{dt} = 2k_1 n_e - k_2 [O] N^2 - k_4 \left[O_3^*\right] [O] N - k_5 \left[O_3\right] [O] N$$
$$- 2k_6 [O]^2 N^2 - \frac{[O]}{\tau_D}$$

$$\frac{d\left[O_3^*\right]}{dt} = k_2 [O] N^2 - k_3 \left[O_3^*\right] N - k_4 \left[O_3^*\right] [O] N - \frac{\sigma \left[O_3^*\right]}{\tau_D} - \frac{\left[O_3^*\right]}{\tau_R}$$

$$\frac{d\left[O_3\right]}{dt} = k_3 \left[O_3^*\right] N - k_5 \left[O_3\right] [O] N + \frac{\sigma \left[O_3^*\right]}{\tau_D} + \frac{\left[O_3^*\right]}{\tau_R}$$

Whence in steady state

$$[O] = \frac{2k_1 n_e}{k_2 N^2 + k_4 \left[O_3^*\right] N + k_5 \left[O_3\right] N + 2k_6 [O] N^2 + \tau_D^{-1}}$$

$$\left[O_3^*\right] = \frac{k_2 [O] N^2}{k_3 N + k_4 [O] N + \sigma \tau_D^{-1} + \tau_R^{-1}}$$

$$\left[O_3\right] = \frac{k_3 \left[O_3^*\right] N + \left[O_3^*\right] \sigma \tau_D^{-1} + \left[O_3^*\right] \tau_R^{-1}}{k_5 [O] N}$$

---

* Vibrationally excited.

8

where P is the pressure in Torr and α varies monotonically with time from 1 to 2,

$$[O_3^*] = 1 \times 10^{-3} \, P \, [O] , \qquad (10)$$

$$[O_3] = 3.3 \times 10^{-3} \, P . \qquad (11)$$

In Equation (9) the 1 in the denominator results from the recombination of O-atoms on the walls of the discharge tube. For non-catalytic walls ($\gamma \approx 0$ for Reaction 7), Equation (9) becomes

$$[O] = \frac{3 \, k_1 \, n_e}{\alpha \, P^2} \quad \text{(non-catalytic wall)} . \qquad (12)$$

Thus, for $P = 0.1$ Torr, $k_1 = 2 \times 10^{-11}$ and arbitrarily taking $n_e \equiv 2 \times 10^7$ cm^{-3} we find for catalytic walls

$$
\begin{aligned}
[O] &= 1.2 \times 10^{-4} \\
[O_3^*] &= 1.2 \times 10^{-8} \\
[O_3] &= 3.3 \times 10^{-4}
\end{aligned}
\qquad (13)
$$

Note that $[O_3^*] / [O_3] = 4 \times 10^{-5}$, which is considerably smaller than the thermal equilibrium population at $300°$ K, where $[O_3^*] / [O_3] = 6.7 \times 10^{-3}$. For non-catalytic walls,

$$
\begin{aligned}
[O] &= 1.2 \times 10^{-1} \\
[O_3^*] &= 1.2 \times 10^{-5} \\
[O_3] &= 3.3 \times 10^{-4} .
\end{aligned}
\qquad (14)
$$

The steady state mole fraction of ozone $[O_3]$ is independent of $[O]$ (and hence wall catalycity) because O_3 is made by O-atoms (Reactions 2 and 3), but it is also destroyed by O-atoms (Reaction 5). On the other hand, O_3^* is made by O-atoms (Reaction 2) but it is destroyed by O_2-molecules (Reaction 3) and hence $[O_3^*]$ scales like $[O]$.

---

*Vibrationally excited.

Time History

Approximate time histories for $[O]$, $[O_3^*]$ and $[O_3]$ are shown for the catalytic case in Figure 2. Here the slopes $(d[X]/dt)$ are established by the dominant term(s) in the differential equations of Table 2, whereas steady state levels are approached at about 3 destruction times given by the dominant negative term(s). It should be noted that O reaches steady state in about 0.4 sec but O_3 takes 15 minutes.

Radiation Predictions

The IR radiation emitted in the instrument band pass $(\Delta \lambda_{B.P.} = 10^{-3} \mu)$ by the O_3^* can be approximately calculated from the equation

$$I_{O_3^*} = \frac{\left[O_3^*\right] N}{4 \pi \tau_{RAD}} \cdot \frac{hc}{\lambda} \cdot 1 \cdot \frac{\Delta \lambda_{B.P.}}{\Delta \lambda_{Band}} \cdot \qquad (15)$$

For the experimental conditions with catalytic walls, we have:

$$I_{O_3^*} = \frac{1.2 \times 10^{-8} \times 3.5 \times 10^{15}}{4 \pi \times 0.1} \cdot \frac{hc}{\lambda} \cdot 3 \times 10^3 \times \frac{10^{-3}}{1} \qquad (16)$$

$$= 2 \times 10^{-12} \text{ watts/cm}^2 \text{ - ster.}$$

For non-catalytic walls, $I_{O_3^*}$ would be 10^3 times larger.

These intensities must be compared with the threshold sensitivity of the IR optical system which is part of the experimental facility

$$I_{threshold} \approx 4 \times 10^{-8} \text{ watts/cm}^2 \text{ ster.} \qquad (17)$$

Hence, it is seen that the present system misses seeing the discharge produced IR signal by about 4 orders of magnitude. Even if the walls of the discharge tube were made non-catalytic to O-atoms the system would still be inadequate. We believe our calculations of $[O_3^*]$ to be an upper bound.

It should be pointed out that nothing much can be gained by varying the pressure. Note that for the non-catalytic wall case (Equations (10) and (12))

$$\left[O_3^*\right] = \frac{3 \times 10^{-3} k_1 n_e}{\alpha P}, \quad \text{for } [O] << \left[O_2\right] \qquad (18)$$

---
*Vibrationally excited.

10
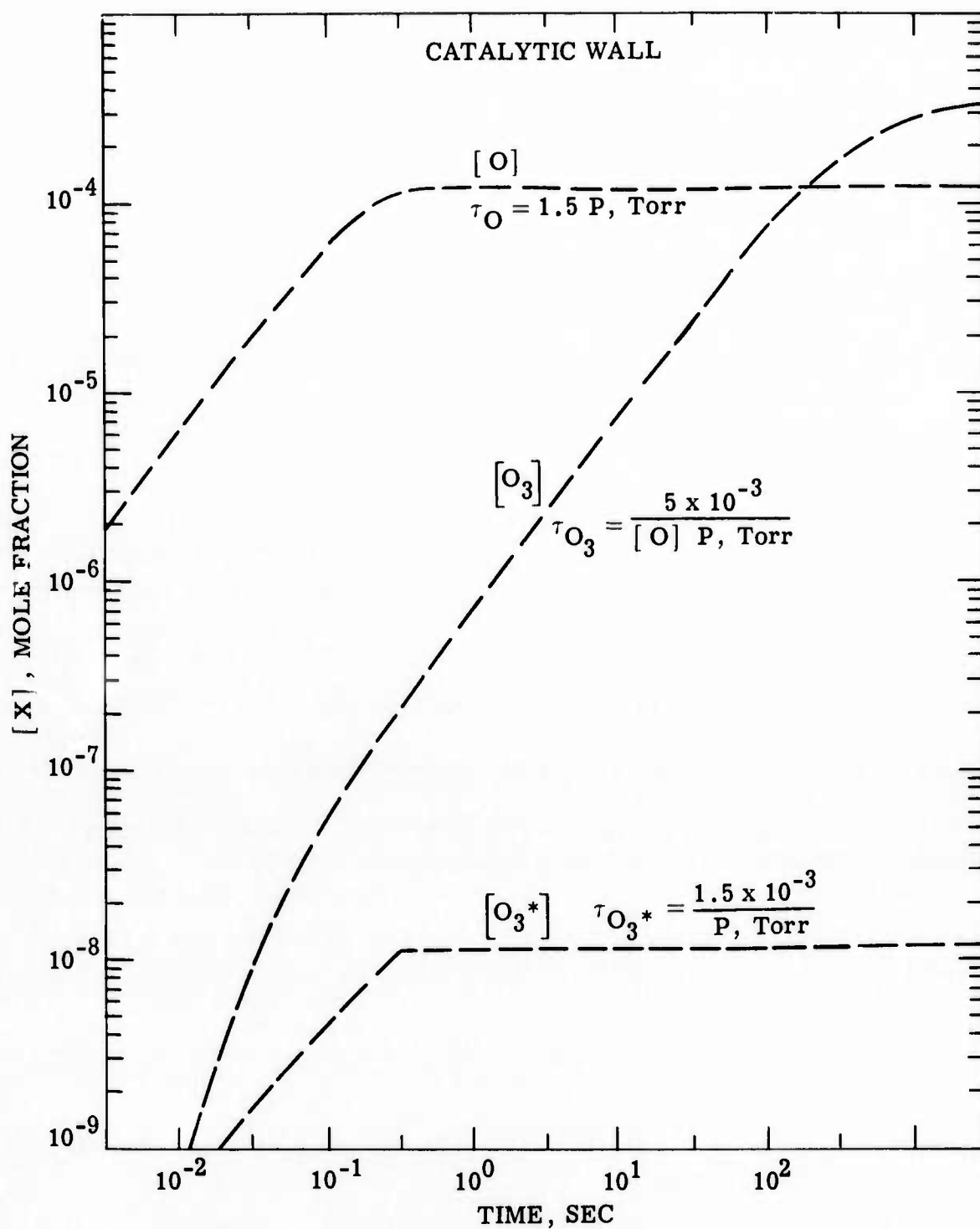
Figure 2. Species history during discharge.

Pure O_2, $P = 0.1$ Torr, $n_e = 2 \times 10^7$ cm^{-3}, $k_1 = 2 \times 10^{-11}$ cm^3 sec^{-1}

11

so that

$$I_{O_3^*} \propto \left[O_3^*\right] N \propto n_e . \tag{19}$$

Hence it seems that the signal could only be increased by increasing n_e, but note that Equation (12) gives

$$[O] \propto \frac{n_e}{P^2} . \tag{20}$$

which, for an assumed n_e of 2×10^7 was already about as large as allowable ($[O] \gtrsim 0.1$). We therefore conclude that a signal gain would only be accomplished by simultaneously increasing n_e and P such that $[O] \approx$ constant. This is probably not possible to do.

$$e + O_3 \rightarrow e + O_3^*$$
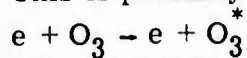
As already mentioned above, the rate constant for Reaction 14 is not known. For the conditions considered above, however, it is readily shown that Reaction 14 would dominate the O_3^* production only if

$$k_{14} \gtrsim 10 \ k_1 \quad \text{(catalytic wall)} \tag{21}$$

$$k_{14} \gtrsim 10^4 \ k_1 \quad \text{(non-catalytic wall) .} \tag{22}$$

It is most unlikely that $k_{14} \gtrsim 10^{-9}$, hence Equation (22) can not be achieved and Reaction 14 is unlikely to affect the conclusions reached above.

Finally, let us ask if the present experiment could be modified to measure the rate of Reaction 14. Suppose pure O_3 were used as the test gas in the discharge tube, then, an upper bound to steady state $[O_3^*]$ is given by

$$\left[O_3^*\right] = \frac{k_{14} \ n_e}{k_3^{\prime} \ N} \tag{23}$$

where $k_3^{\prime} \equiv k_3 = 2 \times 10^{-14}$, $P = 0.1$ Torr of O_3, $n_e \equiv 2 \times 10^7$ (upper bound), and $k_{14} \lesssim 1 \times 10^{-9}$, we find that

$$\left[O_3^*\right] \lesssim 3 \times 10^{-4} . \tag{24}$$

---

* Vibrationally excited.

12

This $[O_3^*]$ is about 4 orders of magnitude larger than that predicted for the case where O_2 is the test gas. However, that case produced insufficient O_3^* by about a factor of 10^4. Considering that Equation (24) represents an unlikely upper bound, the O_3 test gas experiment is not considered likely to succeed. In any case, the $[O_3^*]$ concentration shown in Equation (24) would be less than room temperature thermal concentration.

---

*Vibrationally excited.

PART II

EXPERIMENTAL PROGRAM

J. Strong and P. Hansen

Astronomy Research Facility
University of Massachusetts
Amherst, Massachusetts

Experimental Facility

The discharge column was contained in a large steel absorption cell 1 meter
in diameter and 30 meters long. The inside of the cell is normally coated with
a nonconductive epoxy paint. Thus, a 12-meter section in the center of the cell
was coated with conductive paint. This formed the outer electrode. The inner
electrode was a 7.5 cm diameter 12 meters long aluminum tube centrally
suspended in the cell. By triple passing the cell, the effective optical path-
length (Figure 3) of the discharge column was 36 meters.

The discharge was powered by a 5 Kw electronically controlled power
supply. Modes of operation included either d.c. or 60 Hz a.c. Good steady
discharges were obtained in the 0.05 to 0.35 Torr pressure range. Alternating
current discharges were more stable than d.c. discharges due to arc suppres-
sion. A Langmuir probe was used to sample electron temperatures when the
discharge was operated in the d.c. mode. Electron temperatures in all cases
where a discharge could be maintained were found to lie in the range of 0.5 to
2.5 ev. A residual gas analyzer was used to monitor impurities in the discharge

The spectroscopic equipment included a Hadamard transform spectrometer
(Reference 1) (used in the single scan mode) covering the wavelength range
from 6 to 21 microns, a Brower M10 monochromator, and a Perkin-Elmer
210B monochromator. The latter two instruments were used to cover the 1 to 4
micron wavelength range. Both monochromators were modified for use with
cooled PbS detectors.

Measurements

Our emphasis has been on attempts to observe excited ozone O_3^* in air and
oxygen discharges. The discharge was excited with both direct and alternating

---

1. P. Hansen and J. Strong, Appl. Opt. 11 , 502 (March 1972).
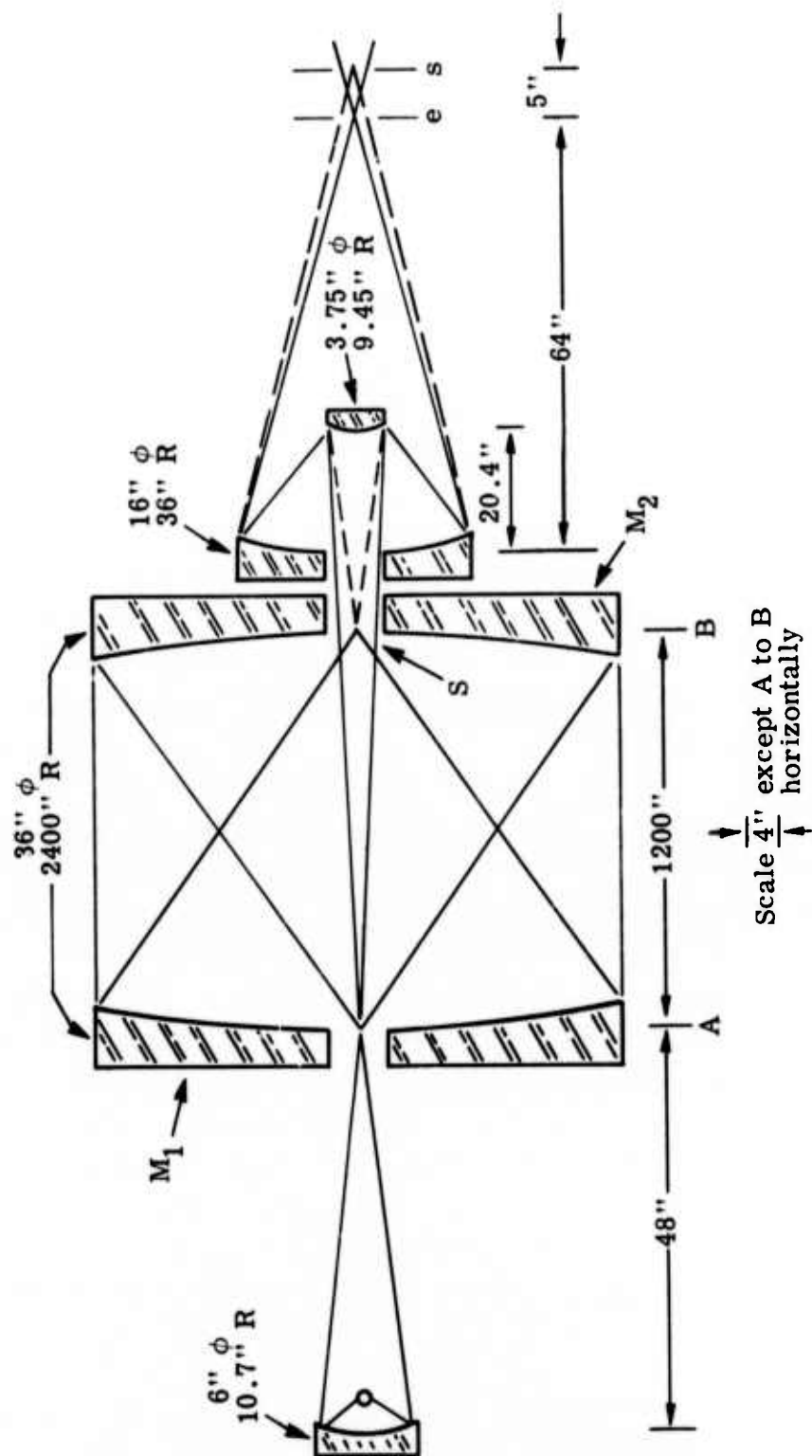
* Vibrationally excited.

14

Figure 3. Optical path in the 30-meter absorption cell.

15

current between the outer wall and a central electrode. This discharge configuration required a conductive outer wall which was catalytic--such that, as pointed out in the analysis by Wray (appended), it reduced the O_3^* concentration by an estimated three orders of magnitude (as compared to glass walls).

Background radiation causes a serious problem because the optics of the discharge column are at room temperature $\sim 290K$. This is true especially for the 9.6μ ozone band, a wavelength where the 290K blackbody curve peaks. The O_3^* concentration could be increased by increasing number density of electrons and gas pressure, simultaneously. With the present catalytic walls and discharge configuration, this could be done by employing a thermionic central electrode. The resulting gain in the O_3^* concentration is not, however, judged enough to bring success--at most, one order of magnitude.

Other methods of exciting discharges for the ozone studies have been considered. One would be to make the outside wall non-catalytic. Others include RF and spark gap discharges in order to enhance very greatly number densities at higher pressures. RF discharges did not appear feasible for us. Spark and continuous discharges using low surface area auxiliary internal electrodes appear to have some merit, but would have required considerable alterations of the present discharge configuration.

The best use of the present system lies in the wavelength range below 4μ where background radiation is less pronounced. To explore here, we have taken spectra of oxygen, nitrogen, and air discharges using a circularly variable filter for low resolution spectra, and the grating monochromators for better resolution ($\Delta\nu \sim 5$ cm^{-1}). Pressures ranged from .05 to .35 Torr.

Typical monochromator spectra are shown in Figure 2. The spectra were obtained with a.c. discharges with total currents near 3 amperes and pressure near .25 Torr. These conditions optimized the signal-to-noise ratio. Higher pressures caused non-radiative dark spaces in the discharge column reducing the effective optical cross section. At lower pressures $p < 0.1$ Torr, necessary current densities could not be obtained to generate appreciable signals.

The oxygen spectrum shows the atomic oxygen lines previously seen by Saum and Benesch (Reference 2). Line 4 in the spectrum is a previously

2. K.A. Saum and W.M. Benesch, Appl. Opt. 9, 1419 (June 1970).

    * Vibrationally excited.

unobserved atomic oxygen line. The nitrogen spectra show the presence of CO with some as yet unidentified species near 2.10 and 2.45 microns. The air spectra are similar to the nitrogen spectra with less s/n.

Near the termination of this contract, a cooperative effort was undertaken with R. Murphy of AFCRL, Bedford, Massachusettes, to obtain spectra of the 12-meter discharge column in the 1 to 6 micron wavelength region using an interferometer and cooled PbS and PbSe detectors. Background signal problems were reduced by using a pulsed discharge on the chopper.

PART III

EPILOGUE*

The effort described in the preceding portions of this report was originally conceived and begun in order to rapidly acquire certain information concerning the properties of irradiated air-like gaseous mixtures, using an already existing, operable laboratory device.

Unfortunately, this effort was mitigated by time, circumstances, and other more productive programs. Consequently, this laboratory endeavor was terminated in early calendar 1974 by mutual but reluctant agreement of all parties involved.

The efforts of all personnel on this project were most commendable throughout its brief existence.

---

*Added in press by the Defense Nuclear Agency's Contracting Officers Representative.